American Journal of Electrical Power and Energy Systems
2025; 14(3): 45-63
http://www.sciencepublishinggroup.com/j/epes
doi: 10.11648/j.epes.20251403.11
ISSN: 2326-912X (Print); ISSN: 2326-9200 (Online)

Analysis of Dynamic Interactions Between Reactive Compensation and Voltage Stability in THT Networks with SVC

Amos Omboua Eyandzi[1, *], Rodolphe Gomba[1], Nianga-Apila[1], Timothee Nsongo[2], Ursula Vanelie Kani Mboyo[1]

[1]Polytechnic Superior National School (ENSP), Marien Ngouabi University, Brazzaville, Congo
[2]Faculty of Sciences and Techniques, Marien Ngouabi University, Brazzaville, Congo

Email address:

ombouaweb@gmail.com (Amos Omboua Eyandzi), gombarodolphe@gmail.com (Rodolphe Gomba), apilanianga@gmail.com (Nianga-Apila), nsongo@yahoo.com (Timothee Nsongo), ur-sulakani2022@gmail.com (Ursula Vanelie Kani Mboyo)
*Corresponding author

To cite this article:

Amos Omboua Eyandzi, Rodolphe Gomba, Nianga-Apila, Timothee Nsongo, Ursula Vanelie Kani Mboyo. (2025). Analysis of Dynamic Interactions Between Reactive Compensation and Voltage Stability in THT Networks with SVC. *American Journal of Electrical Power and Energy Systems, 14*(3), 45-63. https://doi.org/10.11648/j.epes.20251403.11

Received: 13 May 2025; **Accepted:** 18 April 2025; **Published:** 3 June 2025

Abstract: This paper investigates the impact of inte-grating a 35 MW industrial load into an electrical transmission network, with a focus on the role of the Static Var Compensator (SVC) in voltage regulation and system performance enhancement. The added load induces a voltage drop below 0.9 p.u., threatening dynamic stability and potentially triggering unwanted phenomena such as electromechanical oscillations or protective device misoperations. These disturbances are further exacerbated by a decrease in the power factor due to increased phase shift between voltage and current, leading to higher system losses. The SVC demonstrates high effectiveness in mitigating these effects by dynamically injecting reactive power and restoring voltage levels close to nominal values. Its thyristor-controlled operation provides fast and adaptive compensation, outperforming traditional fixed capacitors and reactors in transient response. Using real-world data from the Congolese power grid, this study employs simulation-based scenarios to evaluate the SVC's performance under local operating conditions. Results confirm that optimised reactive power com-pensation enhances grid reliability and facilitates the integration of heavy industrial loads. Recommendations are proposed for efficient SVC deployment in developing electrical infrastructures.

Keywords: Network Stability, SVC, Reactive Power Compensation, Congolese Power Grid, FACTS, Dynamic Simulation

1. Introduction

The interconnection of THT electrical networks is essential for ensuring the reliability and efficiency of electricity supply on both regional and national scale. However, these complex networks face significant challenges in maintaining voltage stability, especially during disturbances and load variations. Reactive power compensation is crucial for maintaining appropriate voltage levels and preventing voltage collapse. Traditionally achieved through passive means, this compensation has shown its limitations as electrical networks evolve. [2, 11].

Flexible power electronics systems for alternating current transmission systems (FACTS), including static VAR compensators (SVCs), offer promising solutions for reactive compensation and improving voltage stability in THT networks. SVCs dynamically regulate voltage by rapidly injecting or absorbing reactive power, which is crucial in THT networks where long transmission lines and high loads exacerbate stability prob-lems. [3, 10, 12, 15]. The integration of industrial zone into an THT network presents an additional challenge to the stability and reliability of the electrical system, with loads reaching of up to 35 MW. This article explores the modelling of dynamic effects between reactive power compensation and voltage stability in THT networks, focusing on the use of SVCs. We argue that effective reactive power

compensation through an SVC can significantly improve voltage stability, even with the integration of large industrial loads. To support this thesis, we will analyse several key aspects: reactive power compensation with an SVC, the voltage magnitude and phase, injected active and reactive power, as well as transmitted and lost power in transmission lines. By combining these elements, we will demonstrate how optimiszd reactive power management can not only stabilize voltage, but also enhance the energy efficiency and reliability of THT networks, particularly when inte-grating large power industrial loads.

2. Methodology

Power system stability is essential to ensure a reliable, high-quality power supply. It can be divided into three categories: transient stability, frequency stability and voltage stability. Transient stability refers to the system's ability to keep generators synchronised after major disturbances. Frequency stability refers to the system's ability to maintain a constant frequency despite variations in load and generation. Finally, voltage stability involves main-taining appropriate voltage levels across the network, often using reactive compensation devices and advanced technologies such as FACTS. [5, 7, 9]

2.1. Stability Analysis Dynamic

The concept of dynamic stability corresponding to small pertubations focuses on analyzing the stability of an electrical system when subjected to slight variations. This analysis is crucial for ensuring that the system remains stable and operates reliably, even in the presence of minor fluctuations. These small disturbances may arise from load variations, changes in energy production, or minor malfunctions within the power grid. The study of small pertubations focuses on the system's responses to these variations to determine its dynamic stability. This concept is particularly important in the analysis of dynamic systems, including fields like fluid mechanics and aeroelasticity. It is based on the idea that, in many physical systems, the responses to change in load or output can be linearized around an equilibrium state. [7, 9]

2.2. Mathematical Modelling

To analyse dynamic stability, we need to model the electrical system. A common model is the linearised model around an equilibrium point. Suppose we have a system described by the following non-linear equations:

$$\frac{dx}{dt} = f(x, u) \tag{1}$$

where x is the state vector, u is the input vector and f is a non-linear function that describes the dynamics of the system.

2.3. Linearisation

To analyse dynamic stability, we need to model the electrical system. A common model used is the linearized model around an equilibrium point. Let us assume that we have a system described by the following non-linear equa-tions:

$$\dot{x} = f(x_0 + \Delta x, u_0 + \Delta u) \tag{2}$$

We apply Taylor expansion of order 1 to the equation2 in Taylor series around the point(x_0, u_0) and neglect terms of order greater than one:

$$f(x_0 + \Delta x, u_0 + \Delta u) \approx f(x_0, u_0) + \frac{\partial f}{\partial x}(x_0, u_0)\Delta u + \frac{\partial f}{\partial u}(x_0, u_0)\Delta u \tag{3}$$

Since $f(x_0, u_0) = 0$ we get:

$$f(x_0 + \Delta x, u_0 + \Delta u) \approx= A\Delta x + B\Delta u \tag{4}$$

The matrices A and B are the Jacobian matrices of the system evaluated at the equilibrium point (x_0, u_0).

$$A = \left.\frac{\partial f}{\partial x}\right|_{(x_0,u_0)} \tag{5}$$

$$B = \left.\frac{\partial f}{\partial u}\right|_{(x_0,u_0)} \tag{6}$$

The linearised system is then described by equation:

$$\dot{\Delta} u = A\Delta x + B\Delta u \tag{7}$$

To calculate the Jacobian matrices A and B, we derive f with respect to each component of x and u. For example, if f is a vector function of n state variables $x_1, x_2 \cdots, u_n$ and r input variables $u_1, u_2 \cdots, u_r$ then:

$$A_{ij} = \left.\frac{\partial f}{\partial x}\right|_{(x_0,u_0)} \tag{8}$$

$$B_{ij} = \left.\frac{\partial f_i}{\partial u_j}\right|_{(x_0,u_0)} \tag{9}$$

Writing these two equations in matrix form gives us

$$A = \begin{vmatrix} \frac{\partial f_1}{\partial x_1} & \cdots & \frac{\partial f_1}{\partial x_n} \\ \cdots & \cdots & \cdots \\ \frac{\partial f_n}{\partial x_1} & \cdots & \frac{\partial f_n}{\partial x_n} \end{vmatrix} \tag{10}$$

$$B = \begin{vmatrix} \frac{\partial f_1}{\partial u_1} & \cdots & \frac{\partial f_1}{\partial u_r} \\ \cdots & \cdots & \cdots \\ \frac{\partial f_n}{\partial u_1} & \cdots & \frac{\partial f_n}{\partial u_r} \end{vmatrix} \tag{11}$$

The analysis of small disturbances is essential to ensure the dynamic stability of electrical systems. By linearising the system around an equilibrium point and studying the

eigenvalues of the Jacobian matrix, we can determine whether the system remains stable in the face of small variations in load or generation. This approach allows us to understand and predict the behaviour of the system under normal operating conditions and to take the necessary measures to maintain the stability of the power system.

3. Application

3.1. SVC (Static VAR Compensator)

A Static VAR Compensator (SVC) is a crucial device in electrical systems, designed to regulate reactive power and maintain voltage stability in transmission networks. By injecting or absorbing reactive power, the SVC helps to stabilize voltage fluctuations and improve the power factor. A typical SVC consists of a thyristor-controlled reactor (TCR) to absorb reactive power, a thyristor-switched capacitor (TSC) to provide reactive power, harmonic filters to mitigate harmonics, and a control system to adjust the output of reactive power output according to the network's needs. [4, 6, 13, 14]

3.2. Modelling SVC Elements

3.2.1. Modelling the TCR Part of the SVC

Let the source voltage be V_s

$$\begin{cases} V_s(t) = V_m \sin(\omega t) \\ L\dfrac{di_{TCR}(t)}{dt} - V_s(t) = 0 \end{cases} \tag{12}$$

With L the inductance of the TCR in the initial condition($\omega t = \alpha$)

$$i_{TCR}(t) = \frac{1}{L}\int_{\frac{\alpha}{\omega}}^{t} V_s(t)dt \tag{13}$$

$$i_{TCR}(t) = -\frac{V_m}{\omega L}(\cos\alpha - \cos\omega t) \tag{14}$$

With α the firing angle in degrees, upon performing a Fourier series analysis, the fundamental component of the current i_{TCR} is given by:

$$i_{1TCR}(t) = A_1 \cos\omega t + B_1 \cos\omega t \tag{15}$$

From equation 12, the current is a function of similarity $i(t) = -i(t)$, so $B_1 = 0$ from which the coefficient A_1 is given by:

$$A_1(t) = \frac{4\omega}{\pi}\int_{\frac{\alpha}{\omega}}^{\frac{\pi}{\omega}} i_{1TCR}(t)\cos\omega t.dt \tag{16}$$

$$A_1(t) = \frac{4\omega}{\pi}\int_{\frac{\alpha}{\omega}}^{\frac{\pi}{\omega}} \frac{V_m}{\omega L}(\cos\alpha - \cos\omega t)\cos\omega t.dt \tag{17}$$

the amplitude of the fundamental current is

$$i_{1TCR}(t) = A_1(t) = \frac{V_m}{\omega L}\left(\frac{2\pi - 2\alpha + \sin 2\alpha}{\pi}\right) \tag{18}$$

With:

$$B_{max}(t) = \frac{1}{\omega L} \tag{19}$$

$$B_{TCR}(\alpha) = B_{max}\left(\frac{2\pi - 2\alpha + \sin 2\alpha}{\pi}\right) \tag{20}$$

Finally, this relationship can be written as:

$$i_{1TCR}(t) = V_m B_{TCR}(\alpha) \tag{21}$$

The relationship between the firing angle α and the conduction angle σ is given by:

$$\alpha + \frac{\sigma}{2} = \pi \tag{22}$$

So the current relationship becomes:

$$i_{1TCR}(\sigma) = V_m B_{max}(\frac{\sigma - sin\sigma}{\pi}) \tag{23}$$

the susceptance of the TCR can be obtained through a linear transformation using the result from equa-tion23, and the matrix that relates the currents and voltages in each branch is given by:

$$\begin{bmatrix} I_{TCR1} \\ I_{TCR2} \\ I_{TCR3} \end{bmatrix} = \begin{bmatrix} -jB_{TCR1} & 0 & 0 \\ 0 & -jB_{TCR2} & 0 \\ 0 & 0 & -jB_{TCR3} \end{bmatrix} \times \begin{bmatrix} V_1 \\ V_2 \\ V_3 \end{bmatrix} \tag{24}$$

The branch voltages and phase voltages are related by the following matrix equation:

$$\begin{bmatrix} V_1 \\ V_2 \\ V_3 \end{bmatrix} = \frac{(\frac{\pi}{6})}{\sqrt{3}} \begin{bmatrix} 1 & -1 & 0 \\ 0 & 1 & -1 \\ -1 & 0 & 1 \end{bmatrix} \times \begin{bmatrix} V_a \\ V_b \\ V_c \end{bmatrix} \tag{25}$$

Similarly, we can write:

$$\begin{bmatrix} I_{TCRa} \\ I_{TCRb} \\ I_{TCRc} \end{bmatrix} = \frac{(\frac{\pi}{6})}{\sqrt{3}} \begin{bmatrix} 1 & -1 & 0 \\ 0 & 1 & -1 \\ -1 & 0 & 1 \end{bmatrix} \times \begin{bmatrix} I_{TCR1} \\ I_{TCR2} \\ I_{TCR3} \end{bmatrix} \tag{26}$$

From equations24, 25 et 26,we obtain:

$$\begin{bmatrix} I_{TCRa} \\ I_{TCRb} \\ I_{TCRc} \end{bmatrix} = \frac{1}{3}\begin{bmatrix} A \end{bmatrix} \times \begin{bmatrix} V_a \\ V_b \\ V_c \end{bmatrix} \tag{27}$$

with A the equation 28

$$\begin{bmatrix} -j(B_{TCR1}+B_{TCR3}) & jB_{TCR1} & -jB_{TCR3} \\ jB_{TCR1} & -j(B_{TCR1}+B_{TCR2}) & jB_{TCR2} \\ jB_{TCR3} & jB_{TCR2} & -j(B_{TCR2}+B_{TCR3}) \end{bmatrix} \tag{28}$$

the susceptances of the three branches of the TCR are the same and we have:

$$\begin{bmatrix} I_{TCRa} \\ I_{TCRb} \\ I_{TCRc} \end{bmatrix} = \frac{1}{3}\begin{bmatrix} -j2B_{TCR} & jB_{TCR} & -jB_{TCR} \\ jB_{TCR} & -j2B_{TCR} & jB_{TCR} \\ jB_{TCR} & jB_{TCR} & -jj2B_{TCR} \end{bmatrix} \times \begin{bmatrix} V_a \\ V_b \\ V_c \end{bmatrix} \tag{29}$$

the equivalent admittances are equal in all the branches of the TCR, then we only have the positive sequence current, which becomes:

$$\bar{I_{TCR}} = jB_{TCR}\bar{V_1} \tag{30}$$

3.2.2. Modelling the TSC Part of the SVC

For the Basic Assumptions, we consider the network to be balanced, meaning the voltages and currents are symmetrical. the thyristors and capacitors are considered to be ideal, with no losses, the thyristors switch instan-taneously without delay, and the system operates in continuous sinusoidal mode. For simplicity, it is assumed that the capacitor is initially discharged. The capacitor is connected to the mains via a thyristor. The voltage V_c across the capacitor and the current I_C through it are given by:

$$I_C(t) = C\frac{dV_c(t)}{dt} \tag{31}$$

where C is the capacitance of the capacitor. The thyristor is controlled to open and close at specific times to regulate the current flow. The switching function $S(t)$ of the thyristor can be modeled by a periodic function:

$$S(t) = \begin{cases} 0 & if \quad the \quad thyristor \quad is \quad open \\ 1 & if \quad the \quad thyristor \quad is \quad closed \end{cases} \tag{32}$$

When the thyristor is closed, the current in the capacitor is determined by the mains voltage:

$$I(t) = S(t).I_c(t) = S(t).C\frac{dV_c(t)}{dt} \tag{33}$$

In sinusoidal conditions, the mains voltage can be represented as:

$$V(t) = V_m \sin(\omega t + \phi) \tag{34}$$

where V_m is the amplitude of the voltage, ω is the angular pulsation, and ϕ is the phase. If the thyristor is closed $(S(t) = 1)$, the differential equation describing the behaviour of the capacitor is:

$$\frac{dV_c(t)}{dt} = \frac{V(t)}{C} \tag{35}$$

By substituting $V(t)$:

$$\frac{dV_c(t)}{dt} = \frac{V_m \sin(\omega t + \phi)}{C} \tag{36}$$

To solve this differential equation, we integrate the two sides:

$$V_c(t) = \frac{V_m}{C}\int \sin(\omega t + \phi)dt \tag{37}$$

The integral of $\sin(\omega t + \phi)$ is:

$$V_c(t) = -\frac{V_m}{C\omega}\cos(\omega t + \phi) + K \tag{38}$$

where K is the constant of integration determined by the initial conditions. If the capacitor is initially uncharged $(V_c(0) = 0)$:

$$V_c(0) = -\frac{V_m}{C\omega}\cos\phi + K \tag{39}$$

So..,

$$K = \frac{V_m}{C\omega}\cos\phi \tag{40}$$

The complete solution is therefore:

$$V_c(t) = \frac{V_m}{C\omega}\left(\cos(\phi) - \cos(\omega t + \phi)\right) \tag{41}$$

For a TSC connected in parallel to the bus i of an electrical network. The reactive power injected by the TSC at the bus i is given by:

$$Q_{TSC} = -\frac{V_i^2}{X_{TSC}} \tag{42}$$

Where V_i is the voltage at bus i and X_{TSC} is the reactance of the TSC capacitor. The reactance X_{TSC} varies as a function the conduction angle α of the thyristors:

$$X_{TSC} = -\frac{X_c}{1 - \frac{\alpha - \sin(\alpha)}{\pi}} \tag{43}$$

with X_C the reactance of the capacitor alone, α the conduction angle of the thyristors, For $(0° \leq \alpha \leq 90°)$, the TSC injects variable reactive power into the network. For $\alpha = 90°$, the TSC is completely blocked and injects no reactive power. In steady state, the total reactive power on the bus i is the sum of

the reactive power of the load and the reactive power injected by the TSC.

$$Q_i = Q_{charge} + Q_{TSC} \tag{44}$$

Mathematical modelling of a TSC using differential equations makes it possible to describe the dynamic behaviour of the capacitor when it is connected to the network via a thyristor, but it also makes it possible to study the impact of the TSC on voltage regulation and reactive power compensation in the electricity network.

3.3. SVC Mathematical Model for Power Flow Calculations

The SVC can be thought of as a variable shunt reactance that automatically adjusts in response to changes in system operating conditions. Depending on the nature of the equivalent reactance of the SVC (i.e. capacitive or inductive), the SVC draws a capacitive or inductive current from the network. Adequate control of this equivalent reactance makes it possible to regulate the amplitude of the voltage at the SVC. They achieve their main operating characteristic at the expense of generating harmonic currents, and filters are used with this type of device.

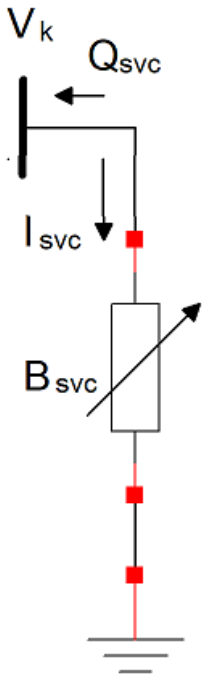

Figure 1. *Simplified SVC model.*

According to figure 1 the current to which the SVC is subjected is as follows.

$$I_{SVC} = jB_{SVC}.V_K \tag{45}$$

The reactive power captured by the SVC, which also corresponds to the reactive power restored to the k bus, is defined by the following equation.

$$Q_{SVC} = Q_k = -V_K^2 B_{SVC} \tag{46}$$

or

$$B_{SVC} = B_C - B_{TCR} \tag{47}$$

With

$$B_C = \frac{1}{X_C} \tag{48}$$

Now the value of B_{TCR} is established by the equation 20, Substituting these equations 20 and 48 we have:

$$B_{SVC} = \frac{1}{X_C.X_L}\{X_L - \frac{X_C}{\pi}[2(\pi - \alpha) + \sin 2\alpha]\} \tag{49}$$

So the reactive power captured by the SVC is given by:

$$Q_{SVC} = \frac{-V_K^2}{X_C.X_L}\{X_L - \frac{X_C}{\pi}[2(\pi - \alpha) + \sin 2\alpha]\} \tag{50}$$

Taking as a starting point the equation 50. The linearity of the SVC equatiaon is formulated as follows:

$$\begin{bmatrix}\Delta P_k \\ \Delta Q_k\end{bmatrix}^{(i)} = \begin{bmatrix}0 & 0 \\ 0 & \frac{\partial Q_k}{\partial \alpha_k}\end{bmatrix}\begin{bmatrix}\Delta\theta_k \\ \Delta\alpha_k\end{bmatrix} \tag{51}$$

where

$$\frac{\partial Q_k}{\partial \alpha_k} = \frac{V_K^2}{\pi X_L}[\cos(2\alpha_k) - 1] \tag{52}$$

4. Results and Discussion

4.1. Network Simulations Under Normal Operating Conditions

Assuming that the network is ideally compensated and that the voltages at the nodes are 220 kV, 110 kV, 30 kV and 20 kV respectively, the simulations were carried out using the system shown in Figure 1. The characteristics of the power stations are given in Table 1, while those of the lines are given in Table 2. These simulations show the variations in active and reactive power that can be transmitted to an infinite power network. The results obtained are illustrated in figure 2. The voltage modules and phases, as well as the injected and absorbed powers are presented in Table 3 and the active and reactive powers transmitted and lost in the lines in Table 5 in Appendix 2.

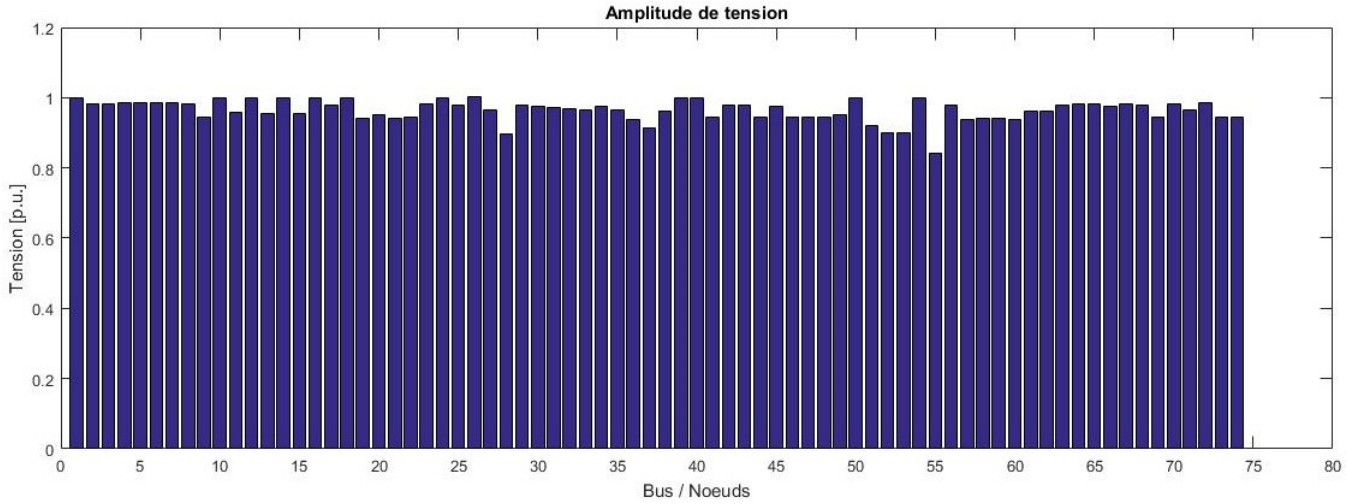

Figure 2. *Networks under normal conditions.*

4.2. Network Simulations Following the Integration of the Industrial Zone

This time, we simulate the system from figure 5, including the integration of the 35MW industrial zone. The simulations are carried out under the same conditions as before. The results obtained are illustrated in Figure 3. The voltage magnitudes and phases, as well as the injected and absorbed powers are presented in Table 6 and the active and reactive powers transited and lost in the lines in Table 7 in Appendix 3.

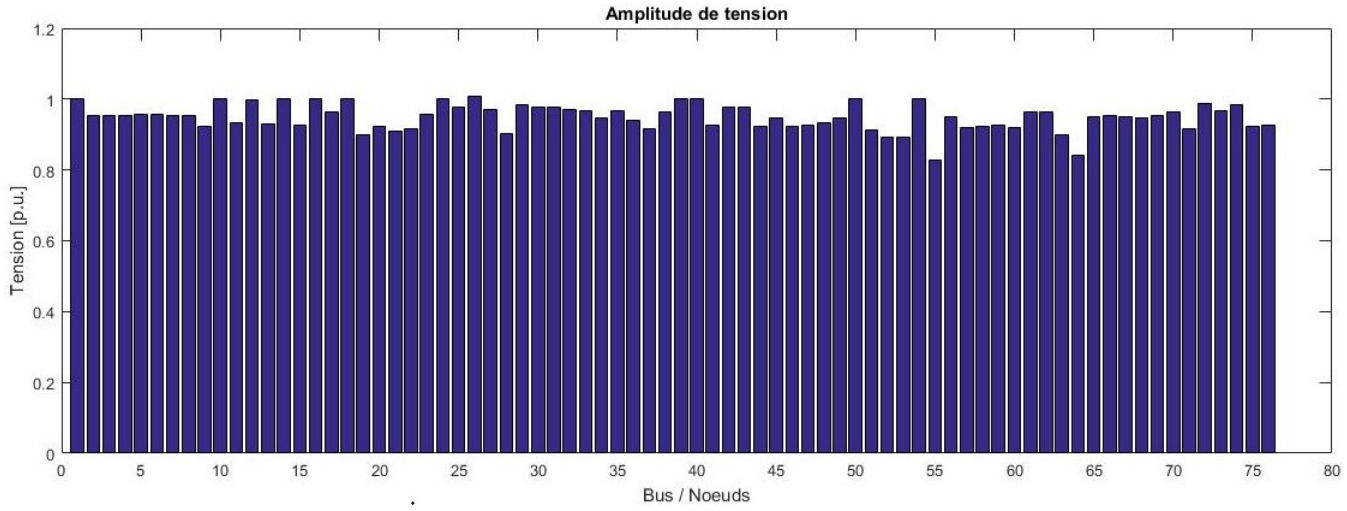

Figure 3. *Network following the integration of the industrial zone.*

A significant drop in voltage has been observed on some nodes, particularly those close to the industrial zone. These voltages are dropping below 0.9 p.u., which may cause instability for some connected equipment. The additional load increases the demand for reactive power, which overloads the existing capacities of generators and transformers. In the absence of compensation devices, this causes significant voltage drops, indicating that the network is not optimised to support such a load.

4.3. Simulation of the Network Including the Industrial Zone, Accounting for the SVC

Here, the simulations take into account the incorporation of the SVC. The results obtained are illustrated in figure 4. The voltage modules and phases, as well as the injected and absorbed powers, are presented in Table 8, and the active and reactive powers transited and lost in the lines in Table 9 in Appendix 4.

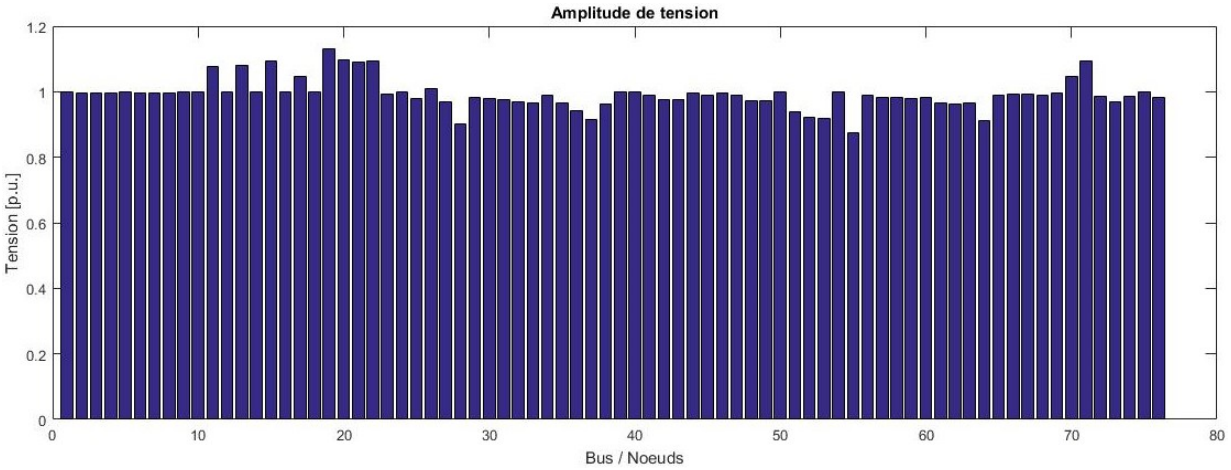

Figure 4. *Network with the industrial estate and the SVC.*

Many studies on power system stability management have already investigated the effectiveness of FACTS devices such as SVC. For example, Hingorani and Gyugyi (2000)[8] demonstrated that the integration of FACTS devices improves the stability of networks under fluctuating loads, focusing mainly on the-oretical simulations without specific studies of industrial areas. Similarly, [16],[17] and [1] have studied the use of devices such as STATCOM and SVC, showing their ability to mitigate voltage drops, but without examining their behaviour in overloaded networks. In contrast to these studies, our paper puts forward an in-depth analysis based on real data from the Congolese network and proposes a practical approach to address the specific prob-lems associated with integrating a 35 MW industrial load. The results show that, without compensation, voltages fall below 0.9 p.u., compromising the overall stability of the network. However, with the integration of an SVC, voltages are restored to around 1 p.u. in real time, demonstrating not only the effectiveness of the device, but also its speed in reacting to dynamic disturbances. Compared to other works, our study includes a more detailed analysis of practical scenarios, taking into account the specific interactions between the industrial load and the critical nodes of the network. Moreover, unlike the studies by Hingorani and Gyugyi, which focused mainly on power flow theories, our simulations clearly show how a device such as the SVC can be used to restore stability in real-life situations.

5. Conclusion

The three figures show a progressive improvement in voltage regulation within the electrical network. This improvement is attributed to the contribution of the SVC, which capable of regulating voltage and better managing power flows to achieve an optimal balance, with voltages close to the nominal value at most of the nodes. The figures highlight a significant evolution in voltage stabilityat network nodes, showcasing a more efficient regulation process, thereby reducing the risk of malfunctions and instability. Continous optimization strategies are necessary to maintain this performance.

Our work provides a unique contribution by combining theoretical and practical analyses tailored to a real-world context, while also demonstrating the specific capabilities of the SVC to stabilize voltages in networks subjected to heavy and dynamic loads. These results represent a significant advancement in the management of developing electrical networks and offer a solid foundation for further improvements in network stability and compensation strategies.

ORCID

0009-0001-3001-8258 (Amos Omboua Eyandzi)
0009-0007-9756-9007 (Nianga-Apila)

Abbreviations

SVC	Static VAR Compensator
MW	Mégawatts
KV	Kilovolts
Pu	per unit
THT	Very High Voltage
FACTS	Flexible AC Transmission Systems
VAR	Volt-Ampere Reactive
TCR	Thyristor-Controlled Reactor
TSC	Thyristor-Switched Capacitor
STATCOM	Static Synchronous Compensator

Acknowledgments

The authors would like to thank the *Supélec* and *Matelek* laboratories for their insightful discus-sions, provision of computing resources, proofreading, valuable advice and technical support. Their contributions were instrumental in the completion of this work.

Author Contributions

Amos Omboua Eyandzi: Conceptualization, Data curation, Formal Analysis, Funding acquisition, Investigation, Methodology, Project administration, Resources, Software, Supervision, Validation, Visualization, Writing - original draft, Writing - review & editing

Conflicts of Interest

The authors declare no conflicts of interest.

Appendix

Appendix I: Data on the Congolese Electricity Network

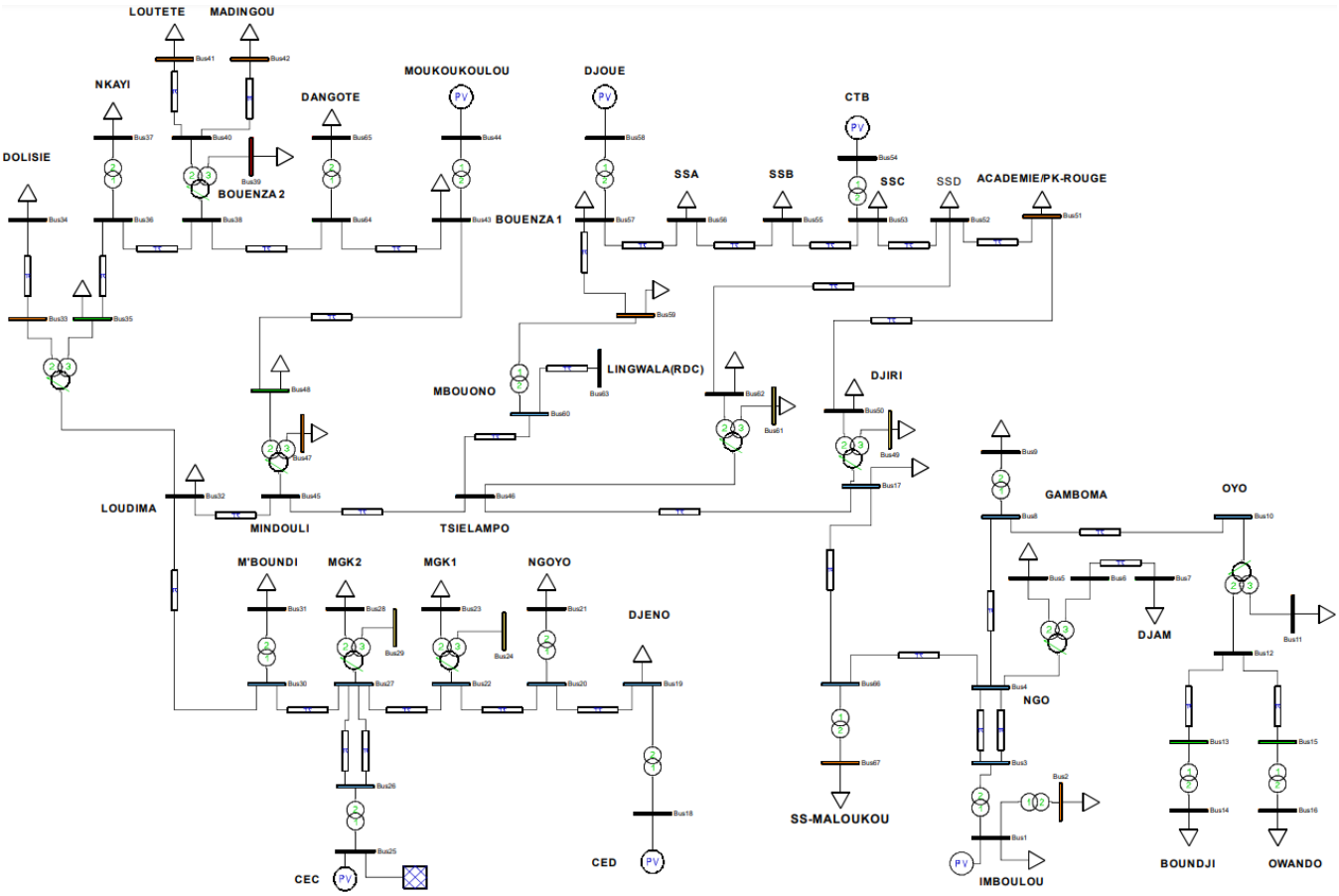

Figure 5. *Congolese network.*

Table 1. *Power plant characteristics.*

Désignation	$U_n(Kv)$	$S_n(MVA)$	$cos\phi$	$P(MW)$	$P(pu)$
CTB	6,6	32,5	0,85	27,62	0,2762
CEC	15,75	352,941	0,85	300	3
Moukoukoulou	10,5	88,235	0,85	75	0,75
Imboulou	10,5	150	0,85	120	1,2
Djou?	5,5	18,8	0,85	15	0,15

Table 2. *Line characteristics.*

N°	Ligne	$U_n(kv)$	$R(pu)$	$X(pu)$	N°	Ligne	$U_n(kv)$	$R(pu)$	$X(pu)$
01	IMB-NGO	220	0,015	0,067	18	OYO-BNDJ	110	0,128	0,316
02	NGO-GAM	220	0,009	0,063	19	LOUD-NKAYI	110	0,34	0,085
03	GAM-OYO	220	0,010	0,073	20	NKAYI-BOUE2	110	0,079	0,195
04	DJEN-NGY	220	0,002	0,008	21	BOUE2-DGT	110	0,046	0,140
05	MKB1-NGY	220	0,002	0,011	22	DGT-BOUE1	110	0,046	0,140
06	MKB2-MKB1	220	0,0005	0,003	23	MIMD-BOUE1	110	0,100	0,289
07	MKB2-MBOU	220	0,004	0,032	24	LOUD-DOL	30	O,117	0,333
08	CEC-MKB2	220	0,001	0,014	25	BOUZ2-LOUT	30	0,69	0,68
09	LOUD-MBOU	220	0,016	0,115	26	BOUZ2-MADI	30	2,3	1,14
10	LOUD-MIND	220	0,018	0,130	27	MBOUO-DJOUE	30	0,055	0,146
11	MIND-TSIE	220	0,012	0,088	28	DJOUE-SSA	30	0,122	0,244
12	TSIE-DJIRI	220	0,002	0,018	29	SSA-SSB	30	0,101	0,086
13	MBOUO-TSIE	220	0,002	0,011	30	SSB-SSC	30	0,097	0,163
14	MBOUO-RDC	220	0,003	0,12	31	SSC-SSD	30	0,101	0,8
15	NGO-DJIRI	220	0,024	0,173	32	SSD-PK.AC	30	0,43	0,61
16	NGO-DJAM	110	0,117	0,333	33	PK.AC-DJIRI	30	0,075	0,2
17	OYO-OWDO	110	0,046	0,323	34	SSD-TSIE	30	0,075	0,2

Appendix II: Evaluation Under Normal Conditions

This appendix provides a detailed assessment of the results obtained in normal operating situations.

Table 3. *Line flow Under Normal Conditions.*

Bus	V	Phase[rad]	P gen	Q gen	P load	Q load
Bus1	1.00000	−0.85980	1.20000	0.17826	0.00300	0.00100
Bus10	0.98354	−1.15509	0.00000	−0.00000	0.00000	0.00000
Bus10(twt)	0.98365	−1.15849	−0.00000	−0.00000	0.00000	0.00000
Bus11	0.98277	−1.16065	0.00000	−0.00000	0.04300	0.01300
Bus12	0.98464	−1.15974	0.00000	0.00000	0.00000	0.00000
Bus13	0.98584	−1.16213	0.00000	−0.00000	0.00000	0.00000
Bus14	0.98538	−1.16314	0.00000	0.00000	0.00500	0.00200
Bus15	0.98406	−1.16544	0.00000	−0.00000	0.00000	0.00000
Bus16	0.98245	−1.16889	0.00000	−0.00000	0.01700	0.00700
Bus17	0.94607	−1.34387	0.00000	−0.00000	0.25500	0.05400
Bus17(twt)	0.94559	−1.34956	0.00000	0.00000	0.00000	0.00000
Bus18	1.00000	−0.93636	0.50000	0.21201	0.00000	0.00000
Bus19	0.95761	−1.03875	0.00000	0.00000	0.12300	0.07600
Bus2	0.99912	−0.86136	0.00000	−0.00000	0.00800	0.00400
Bus20	0.95617	−1.04184	−0.00000	0.00000	0.00000	0.00000
Bus21	1.00000	−1.25923	−0.00000	0.96727	1.01200	0.58500
Bus22	0.95488	−1.03350	0.00000	0.00000	0.00000	0.00000
Bus22(twt)	0.97743	−1.03657	0.00000	0.00000	0.00000	0.00000
Bus23	1.00000	−1.03950	−0.00000	0.51111	0.01200	0.05850
Bus24	0.97743	−1.03657	0.00000	−0.00000	0.00000	0.00000
Bus25	1.00000	0.00000	4.06469	2.25771	0.00000	0.00000
Bus26	0.93944	−0.99971	0.00000	−0.00000	0.00000	0.00000
Bus27	0.95314	−1.03094	0.00000	−0.00000	0.00000	0.00000
Bus27(twt)	0.94617	−1.07277	−0.00000	−0.00000	0.00000	0.00000
Bus28	0.94089	−1.11514	−0.00000	0.00000	0.75500	0.00800
Bus29	0.94617	−1.07277	0.00000	−0.00000	0.00000	0.00000
Bus3	0.98225	−1.10251	0.00000	0.00000	0.00000	0.00000

Table 4. *Line flow Under Normal Conditions.*

Bus	V	Phase[rad]	P gen	Q gen	P load	Q load
Bus30	1.00000	−1.11864	0.00000	1.83472	0.00000	0.00000
Bus31	0.97869	−1.27346	−0.00000	0.00000	0.75500	0.00800
Bus32	1.00405	−1.30620	−0.00000	0.00000	0.42200	0.00500
Bus32(twt)	0.98250	−1.32448	0.00000	0.00000	0.00000	0.00000
Bus33	0.96488	−1.34481	−0.00000	0.00000	0.00000	0.00000
Bus35	0.97894	−1.32320	0.00000	0.00000	0.02100	0.01200
Bus36	0.97496	−1.31759	−0.00000	−0.00000	0.00000	0.00000
Bus37	0.97365	−1.32299	0.00000	0.00000	0.02590	0.00500
Bus38	0.96786	−1.29901	0.00000	0.00000	0.00000	0.00000
Bus38(twt)	0.96600	−1.30224	−0.00000	0.00000	0.00000	0.00000
Bus39	0.96560	−1.30361	0.00000	0.00000	0.02600	0.00500
Bus4	0.97642	−1.14407	−0.00000	−0.00000	0.00000	0.00000
Bus4(twt)	0.97713	−1.14478	0.00000	0.00000	0.00000	0.00000
Bus40	0.96454	−1.30412	0.00000	0.00000	0.00000	0.00000
Bus41	0.93901	−1.30928	−0.00000	0.00000	0.02100	0.01400
Bus42	0.91450	−1.29779	−0.00000	0.00000	0.01500	0.01000
Bus43	0.96313	−1.27369	−0.00000	0.00000	0.38300	0.25000
Bus44	1.00000	−1.11946	0.75000	0.20404	0.00000	0.00000
Bus45	1.00000	−1.32854	−0.00000	1.46355	0.00000	0.00000
Bus45(twt)	0.98486	−1.34428	0.00000	0.00000	0.00000	0.00000
Bus46	0.94601	−1.35792	−0.00000	−0.00000	0.00000	0.00000
Bus46(twt)	0.94290	−1.38056	0.00000	0.00000	0.00000	0.00000
Bus47	0.97742	−1.35035	−0.00000	0.00000	0.13000	0.13200
Bus48	0.97734	−1.35432	−0.00000	0.00000	0.42200	0.00000
Bus49	0.94508	−1.35160	−0.00000	−0.00000	0.03700	0.00600
Bus5	0.97712	−1.14488	−0.00000	0.00000	0.00200	0.00000
Bus50	0.94565	−1.35322	−0.00000	−0.00000	0.01300	0.01000
Bus51	0.94549	−1.36623	0.00000	0.00000	0.01300	0.00800
Bus52	0.94572	−1.40514	−0.00000	−0.00000	0.05300	0.04600
Bus53	0.95310	−1.41876	−0.00000	0.00000	0.05300	0.04600
Bus54	1.00000	−1.36321	0.27600	0.22803	0.00000	0.00000
Bus55	0.92069	−1.45782	0.00000	0.00000	0.05300	0.04600
Bus56	0.90159	−1.47731	0.00000	−0.00000	0.05300	0.04600
Bus57	0.90073	−1.52291	0.00000	0.00000	0.12300	0.07600
Bus58	1.00000	−1.49504	0.15000	0.49058	0.00000	0.00000
Bus59	0.84306	−1.52909	−0.00000	−0.00000	0.80000	0.60000
Bus6	0.97785	−1.14538	0.00000	0.00000	0.00000	0.00000
Bus60	0.93919	−1.36518	0.00000	−0.00000	0.00000	0.00000
Bus61	0.94102	−1.38930	0.00000	0.00000	0.15700	0.01900
Bus62	0.94205	−1.39456	−0.00000	0.00000	0.21200	0.02000
Bus63	0.93924	−1.36520	−0.00000	0.00000	0.00000	0.00000
Bus64	0.96297	−1.27948	0.00000	−0.00000	0.00000	0.00000
Bus65	0.96246	−1.28140	−0.00000	−0.00000	0.00900	0.00200
Bus7	0.97873	−1.14961	−0.00000	0.00000	0.01000	0.00300
Bus8	0.98144	−1.14978	−0.00000	−0.00000	0.00000	0.00000
Bus9	0.98093	−1.15163	−0.00000	0.00000	0.00900	0.00200

Table 5. *Active and reactive power transited and lost on the lines Under Normal Conditions.*

Du bus	Au bus	Line	P flow	Q flow	P loss	Q loss
Bus3	Bus4	1.00000	0.58728	−0.05775	0.00538	−0.02393
Bus3	Bus4	2.00000	0.58728	−0.05775	0.00538	−0.02393
Bus27	Bus22	3.00000	0.66555	−0.66386	0.00049	0.00018
Bus26	Bus27	4.00000	1.92425	−1.03304	0.00539	0.06020
Bus26	Bus27	5.00000	1.92425	−1.03304	0.00539	0.06020
Bus30	Bus27	6.00000	−2.37412	1.86219	0.03662	0.26718
Bus30	Bus32	7.00000	1.61316	−0.15451	0.04182	0.20418
Bus33	Bus34	8.00000	0.41487	0.29455	0.01487	0.03455
Bus35	Bus36	9.00000	−0.03849	0.05950	0.00019	−0.00335
Bus36	Bus38	10.00000	−0.06459	0.05770	0.00067	−0.00778
Bus40	Bus41	11.00000	0.02150	0.01432	0.00050	0.00032
Bus40	Bus42	12.00000	0.01589	0.01015	0.00089	0.00015
Bus6	Bus7	13.00000	0.01002	−0.01514	0.00002	−0.01814
Bus38	Bus64	14.00000	−0.12868	0.03561	0.00009	−0.00475
Bus32	Bus45	15.00000	0.74897	−0.75964	0.01890	−0.09479
Bus45	Bus46	16.00000	0.39282	0.52715	0.00568	−0.02942
Bus48	Bus43	17.00000	−0.21617	0.12534	0.00676	0.00352
Bus46	Bus17	18.00000	−0.69004	0.07151	0.00108	−0.00372
Bus50	Bus51	19.00000	0.05169	−0.01774	0.00024	0.00061
Bus52	Bus51	20.00000	−0.03740	0.02784	0.00105	0.00148
Bus53	Bus52	21.00000	−0.01863	0.10586	0.00128	0.00108
Bus55	Bus53	22.00000	−0.23391	−0.03987	0.00644	0.01067
Bus56	Bus55	23.00000	−0.17700	0.00946	0.00390	0.00332
Bus4	Bus8	24.00000	0.07425	−0.11289	0.00013	−0.04895
Bus57	Bus56	25.00000	−0.12123	0.06086	0.00277	0.00541
Bus59	Bus57	26.00000	−0.13802	−0.28095	0.00758	0.02013
Bus46	Bus60	27.00000	0.67107	0.46240	0.00149	0.00021
Bus62	Bus52	28.00000	0.03570	−0.03045	0.00019	0.00050
Bus60	Bus63	29.00000	0.00000	−0.00882	0.00000	−0.00882
Bus64	Bus43	30.00000	−0.13777	0.03834	0.00026	−0.00663
Bus8	Bus10	31.00000	0.06512	−0.06596	0.00006	−0.05749
Bus13	Bus12	32.00000	−0.00500	−0.00201	0.00001	−0.01551
Bus15	Bus12	33.00000	−0.01700	−0.00707	0.00001	−0.01541
Bus4	Bus17	34.00000	1.07753	0.06034	0.02964	0.08242
Bus20	Bus19	35.00000	−0.37373	−0.08124	0.00032	−0.00422
Bus22	Bus20	36.00000	0.65101	−0.23193	0.00104	−0.00248
Bus3	Bus1	37.00000	−1.17456	0.11550	0.01444	0.28875
Bus37	Bus36	38.00000	−0.02590	−0.00500	0.00001	0.00015
Bus43	Bus44	39.00000	−0.74396	−0.08321	0.00604	0.12083
Bus53	Bus54	40.00000	−0.27472	−0.20240	0.00128	0.02563
Bus57	Bus58	41.00000	−0.14737	−0.43794	0.00263	0.05263
Bus60	Bus59	42.00000	0.66958	0.47100	0.00760	0.15196
Bus65	Bus64	43.00000	−0.00900	−0.00200	0.00000	0.00002
Bus14	Bus13	44.00000	−0.00500	−0.00200	0.00000	0.00001
Bus2	Bus1	45.00000	−0.00800	−0.00400	0.00000	0.00002
Bus16	Bus15	46.00000	−0.01700	−0.00700	0.00000	0.00007
Bus9	Bus8	47.00000	−0.00900	−0.00200	0.00000	0.00002
Bus19	Bus18	48.00000	−0.49705	−0.15302	0.00295	0.05899
Bus21	Bus20	49.00000	−1.01200	0.38227	0.01170	0.23405
Bus26	Bus25	50.00000	−3.84850	2.06608	0.21619	4.32379
Bus31	Bus30	51.00000	−0.75500	−0.00800	0.00595	0.11904
Bus4(twt)	Bus4	52.00000	−0.01202	0.01512	0.00000	0.00002
Bus10(twt)	Bus10	53.00000	−0.06504	0.00869	0.00002	0.00022
Bus22(twt)	Bus22	54.00000	−0.01303	0.44236	0.00103	0.01025

Du bus	Au bus	Line	P flow	Q flow	P loss	Q loss
Bus27(twt)	Bus27	55.00000	−0.75822	−0.04020	0.00322	0.03220
Bus32(twt)	Bus32	56.00000	−0.39880	−0.38023	0.00157	0.01573
Bus38(twt)	Bus38	57.00000	−0.06340	−0.02961	0.00003	0.00026
Bus45(twt)	Bus45	58.00000	−0.33632	−0.26218	0.00094	0.00937
Bus17(twt)	Bus17	59.00000	−0.10172	0.00143	0.00006	0.00058
Bus46(twt)	Bus46	60.00000	−0.40519	−0.01343	0.00092	0.00924
Bus5	Bus4(twt)	61.00000	−0.00200	0.00000	0.00000	0.00000
Bus12	Bus10(twt)	62.00000	−0.02203	0.02184	0.00000	0.00005
Bus23	Bus22(twt)	63.00000	−0.01200	0.45261	0.00103	0.01025
Bus28	Bus27(twt)	64.00000	−0.75500	−0.00800	0.00322	0.03220
Bus33	Bus32(twt)	65.00000	−0.41487	−0.29455	0.00139	0.01390
Bus40	Bus38(twt)	66.00000	−0.03738	−0.02447	0.00001	0.00011
Bus48	Bus45(twt)	67.00000	−0.20583	−0.12534	0.00030	0.00304
Bus50	Bus17(twt)	68.00000	−0.06469	0.00774	0.00002	0.00024
Bus62	Bus46(twt)	69.00000	−0.24770	0.01045	0.00035	0.00346
Bus6	Bus4(twt)	70.00000	−0.01002	0.01514	0.00000	0.00002
Bus11	Bus10(twt)	71.00000	−0.04300	−0.01300	0.00001	0.00010
Bus24	Bus22(twt)	72.00000	0.00000	0.00000	0.00000	0.00000
Bus29	Bus27(twt)	73.00000	0.00000	0.00000	0.00000	0.00000
Bus35	Bus32(twt)	74.00000	0.01749	−0.07150	0.00003	0.00028
Bus39	Bus38(twt)	75.00000	−0.02600	−0.00500	0.00000	0.00004
Bus47	Bus45(twt)	76.00000	−0.13000	−0.13200	0.00018	0.00180
Bus49	Bus17(twt)	77.00000	−0.03700	−0.00600	0.00001	0.00008
Bus61	Bus46(twt)	78.00000	−0.15700	−0.01900	0.00014	0.00141

Appendix III: Analysis of the Impact of the Industrial Zone

This appendix presents an exhaustive analysis of the results obtained in the network following the integration of the industrial zone.

Table 6. *Line flow with the impact of the industrial zone.*

Bus	V	Phase[rad]	P gen	Q gen	P load	Q load
Bus1	1.00000	−1.16144	1.20000	0.30523	0.00300	0.00100
Bus10	0.95402	−1.46383	0.00000	−0.00000	0.00000	0.00000
Bus10(twt)	0.95403	−1.46744	0.00000	0.00000	0.00000	0.00000
Bus11	0.95312	−1.46974	−0.00000	0.00000	0.04300	0.01300
Bus12	0.95496	−1.46876	−0.00000	−0.00000	0.00000	0.00000
Bus13	0.95604	−1.47124	0.00000	−0.00000	0.00000	0.00000
Bus14	0.95557	−1.47231	−0.00000	−0.00000	0.00500	0.00200
Bus15	0.95420	−1.47480	0.00000	−0.00000	0.00000	0.00000
Bus16	0.95254	−1.47846	−0.00000	0.00000	0.01700	0.00700
Bus17	0.92277	−1.81526	−0.00000	−0.00000	0.25500	0.05400
Bus17(twt)	0.92277	−1.82089	0.00000	−0.00000	0.00000	0.00000
Bus18	1.00000	−1.28735	0.49993	0.33610	0.00000	0.00000
Bus19	0.93280	−1.39112	0.00013	−0.00000	0.12300	0.07600
Bus2	0.99912	−1.16300	0.00000	−0.00000	0.00800	0.00400
Bus20	0.93037	−1.39413	0.00082	−0.00009	0.00000	0.00000
Bus21	1.00000	−1.61903	0.00039	1.10088	1.01200	0.58500
Bus22	0.92646	−1.38477	0.00059	−0.00007	0.00000	0.00000
Bus22(twt)	0.96322	−1.38955	0.00037	−0.00002	0.00000	0.00000
Bus23	1.00000	−1.39399	0.00017	0.79551	0.01200	0.05850
Bus24	0.96322	−1.38955	0.00000	−0.00000	0.00000	0.00000
Bus25	1.00000	0.00000	4.57100	3.75782	0.00000	0.00000

Bus	V	Phase[rad]	P gen	Q gen	P load	Q load
Bus26	0.89976	−1.34353	0.08433	0.00365	0.00000	0.00000
Bus27	0.92315	−1.38177	0.00552	0.00012	0.00000	0.00000
Bus27(twt)	0.91579	−1.42633	−0.00003	0.00000	0.00000	0.00000
Bus28	0.91027	−1.47153	0.00094	−0.00006	0.75500	0.00800
Bus29	0.91579	−1.42633	−0.00000	−0.00000	0.00000	0.00000
Bus3	0.95731	−1.40923	−0.00000	−0.00000	0.00000	0.00000
Bus30	1.00000	−1.49161	0.00276	2.87801	0.00000	0.00000
Bus31	0.97869	−1.64644	−0.00000	0.00000	0.75500	0.00800
Bus32	1.00838	−1.72810	−0.00000	−0.00000	0.42200	0.00500
Bus32(twt)	0.98671	−1.74666	−0.00000	0.00000	0.00000	0.00000
Bus33	0.96920	−1.76681	0.00000	0.00000	0.00000	0.00000
Bus34	0.90166	−1.81994	−0.00000	−0.00000	0.40000	0.26000
Bus35	0.98292	−1.74583	0.00000	0.00000	0.02100	0.01200
Bus36	0.97830	−1.74091	−0.00000	0.00000	0.00000	0.00000
Bus37	0.97700	−1.74628	0.00000	−0.00000	0.02590	0.00500
Bus38	0.96969	−1.72395	−0.00000	0.00000	0.00000	0.00000
Bus38(twt)	0.96783	−1.72717	0.00000	−0.00000	0.00000	0.00000
Bus39	0.96744	−1.72853	−0.00000	−0.00000	0.02600	0.00500
Bus4	0.94740	−1.45223	0.00000	0.00000	0.00000	0.00000
Bus4(twt)	0.94808	−1.45298	−0.00000	−0.00000	0.00000	0.00000
Bus40	0.96637	−1.72904	−0.00000	−0.00000	0.00000	0.00000
Bus41	0.94090	−1.73418	0.00000	0.00000	0.02100	0.01400
Bus42	0.91644	−1.72274	−0.00000	−0.00000	0.01500	0.01000
Bus43	0.96402	−1.70033	0.00000	−0.00000	0.38300	0.25000
Bus44	1.00000	−1.54619	0.75000	0.19954	0.00000	0.00000
Bus45	1.00000	−1.75875	0.00000	1.84659	0.00000	0.00000
Bus45(twt)	0.98488	−1.77405	0.00000	0.00000	0.00000	0.00000
Bus46	0.92690	−1.82272	0.00000	0.00000	0.00000	0.00000
Bus46(twt)	0.92504	−1.84680	0.00000	−0.00000	0.00000	0.00000
Bus47	0.97744	−1.78012	−0.00000	−0.00000	0.13000	0.13200
Bus48	0.97737	−1.78364	−0.00000	−0.00000	0.42200	0.00000
Bus49	0.92224	−1.82302	0.00000	0.00000	0.03700	0.00600
Bus5	0.94807	−1.45309	0.00000	0.00000	0.00200	0.00000
Bus50	0.92331	−1.82437	0.00000	−0.00000	0.01300	0.01000
Bus51	0.92546	−1.83705	0.00000	0.00000	0.01300	0.00800
Bus52	0.93430	−1.87645	−0.00000	−0.00000	0.05300	0.04600
Bus53	0.94506	−1.89422	0.00000	0.00000	0.05300	0.04600
Bus54	1.00000	−1.83862	0.27600	0.26821	0.00000	0.00000
Bus55	0.91242	−1.93348	0.00000	0.00000	0.05300	0.04600
Bus56	0.89329	−1.95301	0.00000	−0.00000	0.05300	0.04600
Bus57	0.89246	−1.99870	0.00000	0.00000	0.12300	0.07600
Bus58	1.00000	−1.97105	0.15000	0.53190	0.00000	0.00000
Bus59	0.82886	−2.00207	−0.00000	0.00000	0.80000	0.60000
Bus6	0.94877	−1.45362	−0.00000	−0.00000	0.00000	0.00000
Bus60	0.92026	−1.83040	−0.00000	0.00000	0.00000	0.00000
Bus61	0.92312	−1.85588	−0.00000	0.00000	0.15700	0.01900
Bus62	0.92551	−1.86185	−0.00000	0.00000	0.21200	0.02000
Bus63	0.92031	−1.83041	0.00000	0.00000	0.00000	0.00000
Bus64	0.96414	−1.70582	−0.00000	−0.00000	0.00000	0.00000
Bus65	0.96363	−1.70774	0.00000	−0.00000	0.00900	0.00200
Bus66	0.90005	−1.66599	−0.00000	−0.00000	0.00000	0.00000
Bus67	0.84061	−1.75576	−0.00000	0.00000	0.35000	0.21710
Bus7	0.94948	−1.45803	−0.00000	0.00000	0.01000	0.00300
Bus8	0.95212	−1.45823	−0.00000	0.00000	0.00000	0.00000
Bus9	0.95161	−1.46020	0.00000	−0.00000	0.00900	0.00200

Table 7. *Active and reactive power transmitted and lost on the lines with the impact of the industrial zone.*

Du bus	Au bus	Line	P flow	Q flow	P loss	Q loss
Bus3	Bus4	1.00000	0.58698	−0.00028	0.00565	−0.02012
Bus3	Bus4	2.00000	0.58698	−0.00028	0.00565	−0.02012
Bus27	Bus22	3.00000	0.66942	−1.12789	0.00101	0.00348
Bus26	Bus27	4.00000	2.15259	−1.62079	0.00894	0.11105
Bus26	Bus27	5.00000	2.15259	−1.62079	0.00894	0.11105
Bus30	Bus27	6.00000	−2.79693	2.91147	0.06551	0.49910
Bus30	Bus32	7.00000	2.03874	−0.16050	0.06671	0.38264
Bus33	Bus34	8.00000	0.41472	0.29403	0.01472	0.03403
Bus35	Bus36	9.00000	−0.02952	0.06340	0.00018	−0.00339
Bus36	Bus38	10.00000	−0.05560	0.06165	0.00062	−0.00796
Bus40	Bus41	11.00000	0.02149	0.01431	0.00049	0.00031
Bus40	Bus42	12.00000	0.01588	0.01014	0.00088	0.00014
Bus6	Bus7	13.00000	0.01002	−0.01407	0.00002	−0.01707
Bus38	Bus64	14.00000	−0.11964	0.03974	0.00008	−0.00507
Bus32	Bus45	15.00000	1.14082	−0.94771	0.03715	−0.08208
Bus45	Bus46	16.00000	0.77513	0.70907	0.01390	0.03220
Bus48	Bus43	17.00000	−0.22484	0.12614	0.00718	0.00473
Bus46	Bus17	18.00000	−0.32655	0.24359	0.00039	−0.00929
Bus50	Bus51	19.00000	0.04473	−0.02594	0.00023	0.00058
Bus52	Bus51	20.00000	−0.03040	0.03607	0.00110	0.00156
Bus53	Bus52	21.00000	−0.01680	0.14118	0.00229	0.00192
Bus55	Bus53	22.00000	−0.23186	−0.04071	0.00646	0.01069
Bus56	Bus55	23.00000	−0.17497	0.00860	0.00388	0.00331
Bus4	Bus8	24.00000	0.07425	−0.10470	0.00012	−0.04606
Bus57	Bus56	25.00000	−0.11924	0.05993	0.00273	0.00533
Bus59	Bus57	26.00000	−0.13403	−0.31057	0.00916	0.02432
Bus46	Bus60	27.00000	0.67515	0.43509	0.00151	0.00063
Bus62	Bus52	28.00000	0.04211	−0.05604	0.00043	0.00115
Bus60	Bus63	29.00000	0.00000	−0.00847	0.00000	−0.00847
Bus64	Bus43	30.00000	−0.12872	0.04279	0.00024	−0.00672
Bus66	Bus4	31.00000	−1.04410	−0.04684	0.03230	0.11158
Bus8	Bus10	32.00000	0.06512	−0.06066	0.00006	−0.05407
Bus13	Bus12	33.00000	−0.00500	−0.00201	0.00001	−0.01459
Bus15	Bus12	34.00000	−0.01700	−0.00707	0.00001	−0.01448
Bus66	Bus17	35.00000	0.69170	−0.21828	0.01494	−0.01028
Bus20	Bus19	36.00000	−0.37303	−0.19111	0.00040	−0.00359
Bus22	Bus20	37.00000	0.65211	−0.44878	0.00145	0.00023
Bus3	Bus1	38.00000	−1.17396	0.00055	0.01504	0.30077
Bus37	Bus36	39.00000	−0.02590	−0.00500	0.00001	0.00015
Bus43	Bus44	40.00000	−0.74398	−0.07908	0.00602	0.12046
Bus53	Bus54	41.00000	−0.27452	−0.23859	0.00148	0.02962
Bus57	Bus58	42.00000	−0.14695	−0.47082	0.00305	0.06108
Bus60	Bus59	43.00000	0.67364	0.44293	0.00768	0.15350
Bus65	Bus64	44.00000	−0.00900	−0.00200	0.00000	0.00002
Bus67	Bus66	45.00000	−0.35000	−0.21710	0.00240	0.04801
Bus14	Bus13	46.00000	−0.00500	−0.00200	0.00000	0.00001
Bus2	Bus1	47.00000	−0.00800	−0.00400	0.00000	0.00002
Bus16	Bus15	48.00000	−0.01700	−0.00700	0.00000	0.00007
Bus9	Bus8	49.00000	−0.00900	−0.00200	0.00000	0.00002
Bus19	Bus18	50.00000	−0.49630	−0.26352	0.00363	0.07258
Bus21	Bus20	51.00000	−1.01161	0.51588	0.01289	0.25790
Bus26	Bus25	52.00000	−4.22085	3.24524	0.35015	7.00305
Bus31	Bus30	53.00000	−0.75500	−0.00800	0.00595	0.11904

Du bus	Au bus	Line	P flow	Q flow	P loss	Q loss
Bus4(twt)	Bus4	54.00000	−0.01202	0.01405	0.00000	0.00002
Bus10(twt)	Bus10	55.00000	−0.06504	0.00683	0.00002	0.00023
Bus22(twt)	Bus22	56.00000	−0.01418	0.70983	0.00272	0.02716
Bus27(twt)	Bus27	57.00000	−0.75752	−0.04237	0.00343	0.03432
Bus32(twt)	Bus32	58.00000	−0.40761	−0.38349	0.00161	0.01608
Bus38(twt)	Bus38	59.00000	−0.06339	−0.02960	0.00003	0.00026
Bus45(twt)	Bus45	60.00000	−0.32763	−0.26280	0.00091	0.00909
Bus17(twt)	Bus17	61.00000	−0.09476	0.00965	0.00005	0.00053
Bus46(twt)	Bus46	62.00000	−0.41164	0.01173	0.00099	0.00991
Bus5	Bus4(twt)	63.00000	−0.00200	0.00000	0.00000	0.00000
Bus12	Bus10(twt)	64.00000	−0.02203	0.01999	0.00000	0.00005
Bus23	Bus22(twt)	65.00000	−0.01183	0.73701	0.00272	0.02717
Bus28	Bus27(twt)	66.00000	−0.75406	−0.00806	0.00343	0.03432
Bus33	Bus32(twt)	67.00000	−0.41472	−0.29403	0.00138	0.01376
Bus40	Bus38(twt)	68.00000	−0.03738	−0.02446	0.00001	0.00011
Bus48	Bus45(twt)	69.00000	−0.19716	−0.12614	0.00029	0.00287
Bus50	Bus17(twt)	70.00000	−0.05773	0.01594	0.00002	0.00021
Bus62	Bus46(twt)	71.00000	−0.25411	0.03604	0.00038	0.00385
Bus6	Bus4(twt)	72.00000	−0.01002	0.01407	0.00000	0.00002
Bus11	Bus10(twt)	73.00000	−0.04300	−0.01300	0.00001	0.00011
Bus24	Bus22(twt)	74.00000	0.00000	0.00000	0.00000	0.00000
Bus29	Bus27(twt)	75.00000	0.00000	0.00000	0.00000	0.00000
Bus35	Bus32(twt)	76.00000	0.00852	−0.07540	0.00003	0.00030
Bus39	Bus38(twt)	77.00000	−0.02600	−0.00500	0.00000	0.00004
Bus47	Bus45(twt)	78.00000	−0.13000	−0.13200	0.00018	0.00180
Bus49	Bus17(twt)	79.00000	−0.03700	−0.00600	0.00001	0.00008
Bus61	Bus46(twt)	80.00000	−0.15700	−0.01900	0.00015	0.00147

Appendix IV: Impact Analysis of the Iintegration of Industrial Zones with the SVC

This appendix provides a detailed analysis of the results of the network resulting from the integration of the in-dustrial estate, taking into account the SVC.

Table 8. *Line flow with SVC.*

Bus	V	Phase[rad]	P gen	Q gen	P load	Q load
Bus1	1.00000	0.76436	1.20000	0.12696	0.00300	0.00100
Bus10	0.99548	0.47182	0.00000	0.00000	0.00000	0.00000
Bus10(twt)	0.99562	0.46849	0.00000	−0.00000	0.00000	0.00000
Bus11	0.99475	0.46639	0.00000	−0.00000	0.04300	0.01300
Bus12	0.99665	0.46727	−0.00000	−0.00000	0.00000	0.00000
Bus13	0.99789	0.46491	0.00000	0.00000	0.00000	0.00000
Bus14	0.99744	0.46393	−0.00000	0.00000	0.00500	0.00200
Bus15	0.99613	0.46170	−0.00000	0.00000	0.00000	0.00000
Bus16	0.99454	0.45834	0.00000	−0.00000	0.01700	0.00700
Bus17	1.00000	0.15655	−0.00000	0.92322	0.25500	0.05400
Bus17(twt)	0.99811	0.15150	−0.00000	0.00000	0.00000	0.00000
Bus18	1.00000	0.64138	0.49372	−0.38800	0.00000	0.00000
Bus19	1.07756	0.54600	0.01370	−0.00050	0.12300	0.07600
Bus2	0.99912	0.76280	0.00000	−0.00000	0.00800	0.00400
Bus20	1.08087	0.54246	0.09141	−0.00907	0.00000	0.00000
Bus21	1.00000	0.36336	0.03580	0.31591	1.01200	0.58500
Bus22	1.09218	0.54554	0.06703	−0.00748	0.00000	0.00000
Bus22(twt)	1.04612	0.55140	0.03795	−0.00177	0.00000	0.00000

Bus	V	Phase[rad]	P gen	Q gen	P load	Q load
Bus23	1.00000	0.55597	0.01539	−0.86411	0.01200	0.05850
Bus24	1.04612	0.55140	0.00000	−0.00000	0.00000	0.00000
Bus25	1.00000	0.00000	−2.99289	0.35516	0.00000	0.00000
Bus26	1.13227	0.56071	6.12557	6.79036	0.00000	0.00000
Bus27	1.09798	0.54574	0.62783	0.02657	0.00000	0.00000
Bus27(twt)	1.09315	0.51838	−0.00370	0.00162	0.00000	0.00000
Bus28	1.08909	0.49095	0.10075	−0.00606	0.75500	0.00800
Bus29	1.09315	0.51838	0.00000	0.00000	0.00000	0.00000
Bus3	0.99234	0.52364	0.00000	0.00000	0.00000	0.00000
Bus30	1.00000	0.48201	0.25467	−2.72440	0.00000	0.00000
Bus31	0.97869	0.32718	−0.00000	0.00000	0.75500	0.00800
Bus32	1.00814	0.24842	0.00000	0.00000	0.42200	0.00500
Bus32(twt)	0.98647	0.22988	−0.00000	−0.00000	0.00000	0.00000
Bus33	0.96896	0.20972	−0.00000	0.00000	0.00000	0.00000
Bus34	0.90139	0.15657	0.00000	0.00000	0.40000	0.26000
Bus35	0.98269	0.23074	0.00000	−0.00000	0.02100	0.01200
Bus36	0.97811	0.23570	0.00000	0.00000	0.00000	0.00000
Bus37	0.97681	0.23033	−0.00000	0.00000	0.02590	0.00500
Bus38	0.96959	0.25276	−0.00000	0.00000	0.00000	0.00000
Bus38(twt)	0.96773	0.24954	0.00000	−0.00000	0.00000	0.00000
Bus39	0.96733	0.24817	0.00000	−0.00000	0.02600	0.00500
Bus4	0.98815	0.48262	−0.00000	−0.00000	0.00000	0.00000
Bus4(twt)	0.98888	0.48192	−0.00000	−0.00000	0.00000	0.00000
Bus40	0.96627	0.24767	0.00000	0.00000	0.00000	0.00000
Bus41	0.94079	0.24252	−0.00000	−0.00000	0.02100	0.01400
Bus42	0.91633	0.25397	0.00000	−0.00000	0.01500	0.01000
Bus43	0.96397	0.27648	−0.00000	−0.00000	0.38300	0.25000
Bus44	1.00000	0.43062	0.75000	0.19980	0.00000	0.00000
Bus45	1.00000	0.21827	0.00000	1.13419	0.00000	0.00000
Bus45(twt)	0.98488	0.20294	0.00000	−0.00000	0.00000	0.00000
Bus46	0.98904	0.15181	0.00000	−0.00000	0.00000	0.00000
Bus46(twt)	0.98330	0.13141	−0.00000	0.00000	0.00000	0.00000
Bus47	0.97744	0.19688	−0.00000	0.00000	0.13000	0.13200
Bus48	0.97737	0.19333	−0.00000	0.00000	0.42200	0.00000
Bus49	0.99762	0.14967	0.00000	0.00000	0.03700	0.00600
Bus5	0.98887	0.48182	0.00000	−0.00000	0.00200	0.00000
Bus50	0.99672	0.14825	0.00000	−0.00000	0.01300	0.01000
Bus51	0.99066	0.13820	−0.00000	0.00000	0.01300	0.00800
Bus52	0.97199	0.11365	0.00000	−0.00000	0.05300	0.04600
Bus53	0.97161	0.10963	−0.00000	0.00000	0.05300	0.04600
Bus54	1.00000	0.16508	0.27600	0.13561	0.00000	0.00000
Bus55	0.93958	0.07167	0.00000	−0.00000	0.05300	0.04600
Bus56	0.92059	0.05274	−0.00000	−0.00000	0.05300	0.04600
Bus57	0.91936	0.00830	−0.00000	−0.00000	0.12300	0.07600
Bus58	1.00000	0.03661	0.15000	0.39756	0.00000	0.00000
Bus59	0.87480	−0.00336	0.00000	−0.00000	0.80000	0.60000
Bus6	0.98962	0.48133	−0.00000	0.00000	0.00000	0.00000
Bus60	0.98178	0.14538	0.00000	−0.00000	0.00000	0.00000
us61	0.98150	0.12338	−0.00000	−0.00000	0.15700	0.01900
Bus62	0.97968	0.11887	0.00000	−0.00000	0.21200	0.02000
Bus63	0.98184	0.14536	0.00000	−0.00000	0.00000	0.00000
Bus64	0.96407	0.27097	0.00000	0.00000	0.00000	0.00000
Bus65	0.96356	0.26905	−0.00000	0.00000	0.00900	0.00200
Bus66	0.96477	0.28802	0.00000	0.00000	0.00000	0.00000
Bus67	0.91035	0.21071	−0.00000	0.00000	0.35000	0.21710
Bus7	0.99055	0.47718	0.00000	−0.00000	0.01000	0.00300
Bus8	0.99329	0.47702	0.00000	−0.00000	0.00000	0.00000
Bus9	0.99279	0.47521	−0.00000	0.00000	0.00900	0.00200

Table 9. *Active and reactive power transited and lost on the lines with SVC.*

Du bus	Au bus	Line	P flow	Q flow	P loss	Q loss
Bus3	Bus4	1.00000	0.58736	−0.08189	0.00531	−0.02533
Bus3	Bus4	2.00000	0.58736	−0.08189	0.00531	−0.02533
Bus27	Bus22	3.00000	0.41952	2.04874	0.00182	0.00730
Bus26	Bus27	4.00000	1.52092	2.66440	0.00739	0.08227
Bus26	Bus27	5.00000	1.52092	2.66440	0.00739	0.08227
Bus30	Bus27	6.00000	−2.51973	−2.69061	0.05406	0.40274
Bus30	Bus32	7.00000	2.01345	−0.16083	0.06507	0.37089
Bus33	Bus34	8.00000	0.41473	0.29406	0.01473	0.03406
Bus35	Bus36	9.00000	−0.03005	0.06318	0.00018	−0.00339
Bus36	Bus38	10.00000	−0.05614	0.06143	0.00062	−0.00795
Bus40	Bus41	11.00000	0.02149	0.01431	0.00049	0.00031
Bus40	Bus42	12.00000	0.01588	0.01014	0.00088	0.00014
Bus6	Bus7	13.00000	0.01002	−0.01558	0.00002	−0.01858
Bus38	Bus64	14.00000	−0.12018	0.03951	0.00008	−0.00505
Bus32	Bus45	15.00000	1.11770	−0.93608	0.03588	−0.08297
Bus45	Bus46	16.00000	0.75276	0.00921	0.00683	−0.02413
Bus48	Bus43	17.00000	−0.22432	0.12608	0.00715	0.00465
Bus46	Bus17	18.00000	−0.32340	−0.57300	0.00087	−0.00702
Bus50	Bus51	19.00000	0.05361	0.01087	0.00022	0.00054
Bus52	Bus51	20.00000	−0.03967	−0.00131	0.00072	0.00102
Bus53	Bus52	21.00000	−0.02061	0.02024	0.00009	0.00008
Bus55	Bus53	22.00000	−0.23635	−0.04002	0.00631	0.01044
Bus56	Bus55	23.00000	−0.17950	0.00926	0.00385	0.00328
Bus4	Bus8	24.00000	0.07425	−0.11628	0.00013	−0.05015
Bus57	Bus56	25.00000	−0.12375	0.06061	0.00274	0.00535
Bus59	Bus57	26.00000	−0.14422	−0.21227	0.00473	0.01256
Bus46	Bus60	27.00000	0.66485	0.52920	0.00149	−0.00057
Bus62	Bus52	28.00000	0.03416	0.02490	0.00014	0.00037
Bus60	Bus63	29.00000	0.00000	−0.00964	0.00000	−0.00964
Bus64	Bus43	30.00000	−0.12926	0.04254	0.00024	−0.00672
Bus66	Bus4	31.00000	−1.04909	0.05307	0.02874	0.07179
Bus8	Bus10	32.00000	0.06512	−0.06814	0.00006	−0.05890
Bus13	Bus12	33.00000	−0.00500	−0.00201	0.00001	−0.01589
Bus15	Bus12	34.00000	−0.01700	−0.00707	0.00001	−0.01579
Bus66	Bus17	35.00000	0.69704	−0.31111	0.01408	−0.03562
Bus20	Bus19	36.00000	−0.37972	0.53937	0.00075	−0.00398
Bus22	Bus20	37.00000	0.51755	1.02423	0.00223	0.00162
Bus3	Bus1	38.00000	−1.17471	0.16377	0.01429	0.28572
Bus37	Bus36	39.00000	−0.02590	−0.00500	0.00001	0.00015
Bus43	Bus44	40.00000	−0.74398	−0.07931	0.00602	0.12048
Bus53	Bus54	41.00000	−0.27505	−0.11670	0.00095	0.01891
Bus57	Bus58	42.00000	−0.14819	−0.36145	0.00181	0.03611
Bus60	Bus59	43.00000	0.66337	0.53941	0.00758	0.15168
Bus65	Bus64	44.00000	−0.00900	−0.00200	0.00000	0.00002
Bus67	Bus66	45.00000	−0.35000	−0.21710	0.00205	0.04094
Bus14	Bus13	46.00000	−0.00500	−0.00200	0.00000	0.00001
Bus2	Bus1	47.00000	−0.00800	−0.00400	0.00000	0.00002
Bus16	Bus15	48.00000	−0.01700	−0.00700	0.00000	0.00007
Bus9	Bus8	49.00000	−0.00900	−0.00200	0.00000	0.00002
Bus19	Bus18	50.00000	−0.48978	0.46686	0.00394	0.07886
Bus21	Bus20	51.00000	−0.97620	−0.26909	0.01025	0.20508
Bus26	Bus25	52.00000	3.08373	1.46155	0.09084	1.81671
Bus31	Bus30	53.00000	−0.75500	−0.00800	0.00595	0.11904
Bus4(twt)	Bus4	54.00000	−0.01202	0.01556	0.00000	0.00002
Bus10(twt)	Bus10	55.00000	−0.06504	0.00946	0.00002	0.00022

Du bus	Au bus	Line	P flow	Q flow	P loss	Q loss
Bus22(twt)	Bus22	56.00000	0.03709	−0.96694	0.00428	0.04278
Bus27(twt)	Bus27	57.00000	−0.65975	−0.03050	0.00183	0.01825
Bus32(twt)	Bus32	58.00000	−0.40708	−0.38331	0.00161	0.01606
Bus38(twt)	Bus38	59.00000	−0.06339	−0.02960	0.00003	0.00026
Bus45(twt)	Bus45	60.00000	−0.32815	−0.26276	0.00091	0.00911
Bus17(twt)	Bus17	61.00000	−0.10364	−0.02718	0.00006	0.00058
Bus46(twt)	Bus46	62.00000	−0.40362	−0.06846	0.00087	0.00867
Bus5	Bus4(twt)	63.00000	−0.00200	−0.00000	0.00000	0.00000
Bus12	Bus10(twt)	64.00000	−0.02202	0.02261	0.00001	0.00005
Bus23	Bus22(twt)	65.00000	0.00339	−0.92261	0.00426	0.04256
Bus28	Bus27(twt)	66.00000	−0.65425	−0.01406	0.00181	0.01805
Bus33	Bus32(twt)	67.00000	−0.41473	−0.29406	0.00138	0.01376
Bus40	Bus38(twt)	68.00000	−0.03738	−0.02446	0.00001	0.00011
Bus48	Bus45(twt)	69.00000	−0.19768	−0.12608	0.00029	0.00288
Bus50	Bus17(twt)	70.00000	−0.06661	−0.02087	0.00002	0.00025
Bus62	Bus46(twt)	71.00000	−0.24616	−0.04490	0.00033	0.00326
Bus6	Bus4(twt)	72.00000	−0.01002	0.01558	0.00000	0.00002
Bus11	Bus10(twt)	73.00000	−0.04300	−0.01300	0.00001	0.00010
Bus24	Bus22(twt)	74.00000	0.00000	−0.00000	0.00000	0.00000
Bus29	Bus27(twt)	75.00000	0.00000	0.00000	0.00000	0.00000
Bus35	Bus32(twt)	76.00000	0.00905	−0.07518	0.00003	0.00030
Bus39	Bus38(twt)	77.00000	−0.02600	−0.00500	0.00000	0.00004
Bus47	Bus45(twt)	78.00000	−0.13000	−0.13200	0.00018	0.00180
Bus49	Bus17(twt)	79.00000	−0.03700	−0.00600	0.00001	0.00007
Bus61	Bus46(twt)	80.00000	−0.15700	−0.01900	0.00013	0.00130

References

[1] Sarita S Bhole and Prateek Nigam. Improvement of voltage stability in power system by using svc and statcom. International Journal of Advanced Research in Electrical, Electronics and Instrumentation Engineering, 4(2): 76-81, 2015.

[2] Jean-Paul Bouttes. Régulation technique et économique des réseaux électriques. FLUX Cahiers scientifiques internationaux Réseaux et Territoires, 6(2): 43-55, 1990

[3] Pravin Chopade, Marwan Bikdash, Ibraheem Kateeb, and Ajit D Kelkar. Reactive power management and voltage control of large transmission system using svc (static var compensator). In 2011 Proceedings of IEEE Southeastcon, pages 85-90. IEEE, 2011.

[4] Mahdiyeh Eslami, Hussain Shareef, Azah Mohamed, and Mohammad Khajehzadeh. A survey on flexible ac transmission systems (facts). Organ, 1: 12, 2012.

[5] Manel Fergane. Les méthodes damélioration de la stabilit dynamique dans les réseaux electriques. PhD thesis, 2018.

[6] Gabriela Glanzmann. Facts: flexible alternating current transmission systems. Technical report, ETH Zurich, 2005.

[7] Mathurin Gogom, Anedi Oko Ganongo, Nianga Apila, and Desire Lilonga-Boyenga. Optimization of power transit through a double-term line term by the upfc. Science Journal of Energy Engineering, 8(4): 44-53, 2020.

[8] Narain G.. Hingorani and Laszlo Gyugyi. Understanding FACTS: concepts and technology of flexible AC transmission systems. Wiley-IEEE Press, 2000.

[9] Lamia Kartobi. Optimisation de la synthèse des FACTS par les algorithmes: Génétiques et les essaims particulaires pour le contrôle des réseaux électriques. PhD thesis, Ecole Nationale Polytechnique, 2006.

[10] NABM Le, W Mohd Nazmi bin W Musa, Nurlida binti Ismail, Nurul Huda binti Ishak, and Nur Ashida binti Salim. The modeling of svc for the voltage control in power system. Indonesian Journal of Electrical Engineering and Com-puter Science, 6(3): 513-519, 2017.

[11] Pr Cherif.Fetha. Cours qualite de l'energie electrique. Département d'électrotechnique Faculté de Technologie Université Batna 2. Annee 2023/2024.

[12] Mohammed Ahsan Adib Murad, Georgios Tzounas, Muyang Liu, and Federico Milano. Frequency control through voltage regulation of power system using svc devices. In 2019 IEEE Power & Energy Society General Meeting (PESGM), pages 1-5. IEEE, 2019.

[13] Therese Uzochukwuamaka Okeke and Ramy Georgious Zaher. Flexible ac transmission systems (facts). In 2013 international conference on new concepts in smart cities: fostering public and private alliances (SmartMILE), pages 1-4. IEEE, 2013.

[14] Mario-Alberto Rios. Modelisation pour analyses dynamiques des reseaux electriques avec compensateurs de puissance reactive-SVC. PhD thesis, Institut National Polytechnique de Grenoble-INPG, 1998.

[15] Nang Sabai, Hnin Nandar Maung, and Thida Win. Voltage control and dynamic performance of power transmis-sion system using static var compensator. World Academy of Science, Engineering and Technology, 42: 426, 2008.

[16] Arun Singh SENGAR, Raunak CHHAJER, Ghaeth FANDI, and Famous O IGBINOVIA. Comparison of the operational theory and features ofsvc and statcom. 2015.

[17] Nunna Sushma. Comparative analysis of statcom and svc for reactive power enhancement in a long transmission line. International Journal of Computational Science and Engineering, 6(6): 1579-82, 2018.